Lasers in Medical Science
https://doi.org/10.1007/s10103-020-03087-y

ORIGINAL ARTICLE

Histopathological and biomechanical changes in soft palate in response to non-ablative 9.3-μm CO_2 laser irradiation: an in vivo study

Ali H. Badreddine[1] · Stephen Couitt[1] · Charles Kerbage[1]

Received: 6 February 2020 / Accepted: 23 June 2020

Abstract

The purpose of this study was to investigate in vivo the biomechanical and morphological changes in soft palates of Wistar rats from non-ablative irradiation with a 9.3-μm CO_2 laser. A blinded, randomized, controlled study was designed with 45 Wistar rats categorized into treated and control sets. The treated set was exposed to 9.3-μm CO_2 laser irradiation at an average power of 1.0 W and a single pulse fluence of 0.16 J/cm^2 scanned using an automated system at a repetition rate of 315 Hz in a patterned area covering 0.4 cm^2 in 6 s. The tissue of each animal was excised and divided into two halves. One-half was sectioned for histopathology, and the other half was used to measure tissue stiffness, which was reported as the effective Young's modulus. Measurements for both sets were taken at three time points: days 1, 21, and 35. There were no significant adverse events or changes in the behavior of the rats over the duration of the study. The treated set exhibited an order of magnitude increase in stiffness relative to the controls, which was maintained over the three time points. Histopathology showed a moderate contraction/disruption of the lamina propria collagen observed at day 1 and collagen accumulation observed at days 21 and 35 in the tissue remodeling phase. Non-ablative 9.3-μm CO_2 laser irradiation can safely increase oral mucosal stiffness and can be used as an effective treatment to reduce tissue vibrations that are associated with snoring.

Keywords Laser · Oral mucosa · Indentation · Tissue contraction · Snoring · Sleep · Soft palate

Background

The use of lasers to reduce snoring by stiffening the soft palate dates back to 2002 [1] and offers a less invasive alternative to uvulopalatopharyngoplasty. Laser irradiation of the tissue induces a thermal effect that causes a contraction of the tissue beginning at a temperature of around 60 °C [2]. One existing theory for this phenomenon is that heat generated from absorption of laser irradiation causes a disruption of collagen fibril cross-linking, resulting in a rapid contraction of the fibrils into a more entropically favored configuration [2, 3]. This should increase the stiffness of the tissue since the cells and collagen are closer together in a more random arrangement and may form new cross-linking. Additionally, in response to laser irradiation, a scar-like formation over time from an accumulated collagen has been reported in dermal studies and on palatal tissue, which would further increase the tissue stiffness and provide a lasting effect [4–6].

Recently, studies have been reported using an Er:YAG laser [7–9] to reduce snoring by tightening the soft palate with varying reports of efficacy. Er:YAG lasers operate at a wavelength of 2.9 μm and have a strong absorption coefficient (12,800 cm^{-1}) in soft tissues with a penetration depth of only a few microns before a complete absorption of the laser energy occurs [10]. On the other hand, CO_2 lasers have a lower absorption coefficient (800 cm^{-1}), which enables such lasers to induce a deeper tissue effect below the surface [11]. Subsequently, thermal energy generated by CO_2 laser irradiation can reach deeper subepithelial tissues, such as the oral mucosa lamina propria, which has a large concentration of organized collagen and is the primary target of the treatment for snoring, with the aim of causing a longer-lasting effect [12, 13]. Furthermore, with a deeper penetration depth than Er:YAG laser, CO_2 laser irradiation can be less damaging, as the energy penetrates deeper into the tissue and is less likely to cause micro-ablation of the surface during heating and other undesirable effects.

✉ Ali H. Badreddine
abadreddine@convergentdental.com

[1] Convergent Dental, Needham, MA, USA

Published online: 03 July 2020

In this study, we sought to investigate the characteristics of the soft palate at three time points after irradiation with a 9.3-μm CO_2 laser. Histolopathological inflammatory markers and morphological changes in collagen were investigated, along with changes in tissue stiffness as measured by biomechanical indentation. A measurement of the latter was needed to investigate the effect of laser-induced tissue tightening from collagen denaturation (collagen shrinkage and tissue tightening) and from the subsequent wound healing response that generates new collagen. Such a characterization would allow for a better understanding of the tissue contraction and the potential longevity of treatment.

Materials and methods

Animal model

A blinded, in vivo animal study was designed and performed following an IACUC protocol maintained by Toxikon Corporation (Bedford, MA).

Animal types and numbers

There were 45 healthy Wistar rats (*Rattus norvegicus*) used in this study, including males and females (females were non-pregnant and nulliparous). The weight of each rat was at least 250 g with the age approximately 5 weeks old (adult). The animals were purchased from a registered commercial breeder and identified with an ear punch/ear tag. Animals were selected from a larger pool and examined to ensure a lack of adverse clinical signs.

Animal care and handling

The animals were acclimated for a minimum of 5 days, under the same conditions used during the study. Temperature of the room was targeted to be 68 ± 5 °F, with a relative humidity of 30–70%. A minimum of 10 air exchanges per hour was maintained. Lights were set to a 12-h light/dark cycle with full-spectrum fluorescent lights. Animals were housed individually in polycarbonate cages, and laboratory-grade bedding was used as contact bedding. A commercial rodent food was provided ad libitum, along with tap water. The laboratory and animal rooms were maintained as limited access facilities.

Group divisions bases

A total of 45 Wistar rats were used across 3 post-treatment time points (day 1, day 21, and day 35). Time points were based on the characteristics of healing from laser damage corresponding to inflammation (day 1) and tissue remodeling phases (days 21 and 35) [4, 14]. Furthermore, these time points align with three of the time points used in a previous study performed using a radiofrequency ablation system [15]. Each of the three time points consisted of one group of 5 untreated control animals and one group of 10 treated animals, for a total of 15 control animals and 30 treated animals. The untreated control groups were exposed to anesthesia but no laser irradiation. The treated groups were exposed to anesthesia and then were treated with a 9.3-μm CO_2 laser as described below.

Anesthesia procedure

Anesthesia used was ketamine (~ 75 mg/kg) and dexmedetomidine (~ 0.5 mg/kg) delivered through intraperitoneal injection. Prior to the procedure, an injection of buprenorphine (~ 0.03 mg/kg) was administered subcutaneously for analgesia. A second dose of buprenorphine was given to the animals after recovery from anesthesia approximately 8–12 h later.

Postoperative care

Following the treatment, the animals were observed and recorded daily by a trained animal handler (Toxikon, Inc.) for any adverse reactions to the treatment or behavioral changes. Animal weights were measured weekly.

Laser settings and application

A 9.3-μm CO_2 laser (Solea, Convergent Dental, Needham, MA) was used to irradiate the soft palate tissues with a straight handpiece. The diameter of the laser beam was expanded to 2 mm (measured by $1/e^2$ method) and was collimated at the output of the handpiece over a range of 4 cm. The native beam was scanned over the irradiated surface at a pulse scan rate of 315 Hz using a pair of computer-controlled mirrors in a patterned geometry with a uniform spacing of 0.9 mm between centers of each adjacent single laser spot. The pattern covered an area of 0.4 cm^2 in 6 s per location, with an average power of 1.0 W and fluence per pulse of 0.16 J/cm^2. The patterned distribution of pulses was done to prevent an excessive accumulation of heat energy in one location. These settings were empirically determined in vitro on excised cow oral soft palates to achieve a contraction event on the tissue without obvious undesired damage to the superficial tissue structure.

For the treated groups, anesthetized rats were placed on their backs with the mouths held open gently using cotton swabs. Their soft palates were irradiated with the laser in the following sequence. First, irradiation was done on one lateral side of the palate, followed by a delay with no irradiation of ~ 10 s. Then, the opposite lateral side of the palate was irradiated, followed by another ~ 10-s delay. Finally, the central dorsal surface was irradiated. This sequence ensured that the

entire soft palate was completed treated. A 10-s delay was empirically determined to allow the tissue to rapidly cool to sufficiently reduce additive effects from repeated irradiation. The laser application was done in one session at day 0 and was not repeated.

Histopathological examination

At each time point, the corresponding control and treated groups were sacrificed by CO_2 inhalation and the soft palates extracted. Half of each soft palate was blind-labeled and fixed in 10% neutral buffered formalin (NBF) for histopathology. Routine hematoxylin and eosin staining to assess epithelial damage, epithelial healing response, presence and extent of necrosis, and inflammatory infiltrates (granulocytes, macrophages, lymphocytes, plasma cells) was performed by a trained histopathologist. Additionally, Sirius Red staining was done by the histopathologist to study subepithelial collagen density and structure pre- and post-treatment. The initial histopathological scoring descriptions are shown in Table 1.

Table 2 shows a summary of the final histopathological data. Collagen density and organization were combined to provide a quantitative metric of the overall effect on collagen. Inflammation, necrosis, and epithelial effects were also summarized in a similar way. Data for each category was averaged for each group.

Biomechanical stiffness

The other half of each excised soft palate tissue was blind-labeled and placed into a conical tube with PBS (phosphate-buffered saline, Sigma) over an ice pack before processing. The bottom of each sample was dried and placed onto a bead of fast-drying super glue in the dish to keep the surface level with the plate bottom and to prevent the samples from floating or moving during indentation. The glue was air-dried for 30 s. A transfer pipette was then used to place a few drops of saline onto the tissue surface to prevent desiccation. After the last sample was adhered to the dish, PBS was poured into the dish until the samples were completely submerged by 2–3 mm.

The Piuma nanoindenter (Optics 11, Amsterdam, Netherlands) was used with a ~25 μm radius, 0.5 N/m stiffness probe (Optics 11, Amsterdam, Netherlands). The probe, shown in Fig. 1a, was fully submerged in the saline containing the samples, and the optical waveform was then calibrated in the solution. The probe was positioned to contact the bottom surface of the petri dish for calibration of the cantilever. For each measurement, the probe was positioned close to the tissue surface manually by moving the probe at intervals of 50 μm (waveform for this movement without contract shown in Fig. 1b) until contact was achieved with the surface

Table 1 Initial histopathological scoring descriptions

Score	Inflammation	Necrosis	Collagen density	Collagen organization	Re-epithelization	Hyperplasia/ hyperkeratosis
0	None	None	Severely decreased/absent	Absent	Intact epithelium	None
1	Minimal	Epithelial layer - focal	Decreased	Shortened bundles, poor organization	Focal erosion	Minimal
2	Mild	Extending into lamina propria - mild	Normal density	Normal length fibers, poor organization	Extensive erosions ± focal ulceration	Mild
3	Moderate	Extending into lamina propria ± submucosa - moderate	Increased density	Normal length fibers, mostly organized	Multifocal or moderate ulceration	Moderate
4	Severe	Extending into lamina propria + submucosa - marked	Marked increase/consolidation	Normal length fibers, organized as mature tissue	Extensive ulcerations	Severe

Table 2 Simplified histopathological scoring descriptions

Day 1	Day 21	Day 35
Lamina propria inflammatory infiltrates*	Lamina propria inflammatory infiltrates*	Lamina propria inflammatory infiltrates*
Epithelial ulceration*	Epithelial hyperplasia/hyperkeratosis*	Epithelial hyperplasia/hyperkeratosis*
Necrosis*	Necrosis*	Necrosis*
Lamina propria collagen disruption*	Lamina propria fibrosis**	Lamina propria fibrosis**

* Scored on a 0–4 scale (0, normal/none; 1, minimal; 2, mild; 3, moderate; 4, severe/marked)

** Scored on a 0–4 scale (0, none; 1, early; 2, early maturing; 3, late maturing; 4, fully mature)

(waveform for contact with tissue shown in Fig. 1c). Anti-adhesion mode was used due to the adhesive nature of these tissues. The indenter was then reversed 50 μm and then approached with 5-μm intervals until the tip rested just above the tissue surface. The indentation profile was based on values that were established empirically from in vitro work on cow soft palates. This profile used an indentation depth of 15 μm with 3 s to begin the indent, 3 s to hold the indent, and 3 s to remove the indent. The tissue's effective Young's modulus was calculated through the built-in software which used the Hertz model, based on the loading and unloading curves of stress vs strain measured from the cantilever. This was repeated until 10 measurements were made on each sample.

Statistics

Minitab 18 was used to perform statistical analysis on the data. The data appeared to follow a log-normal distribution, which is typical with biomechanical data [16], so statistics were computed on the log-transformed data. Due to differences in

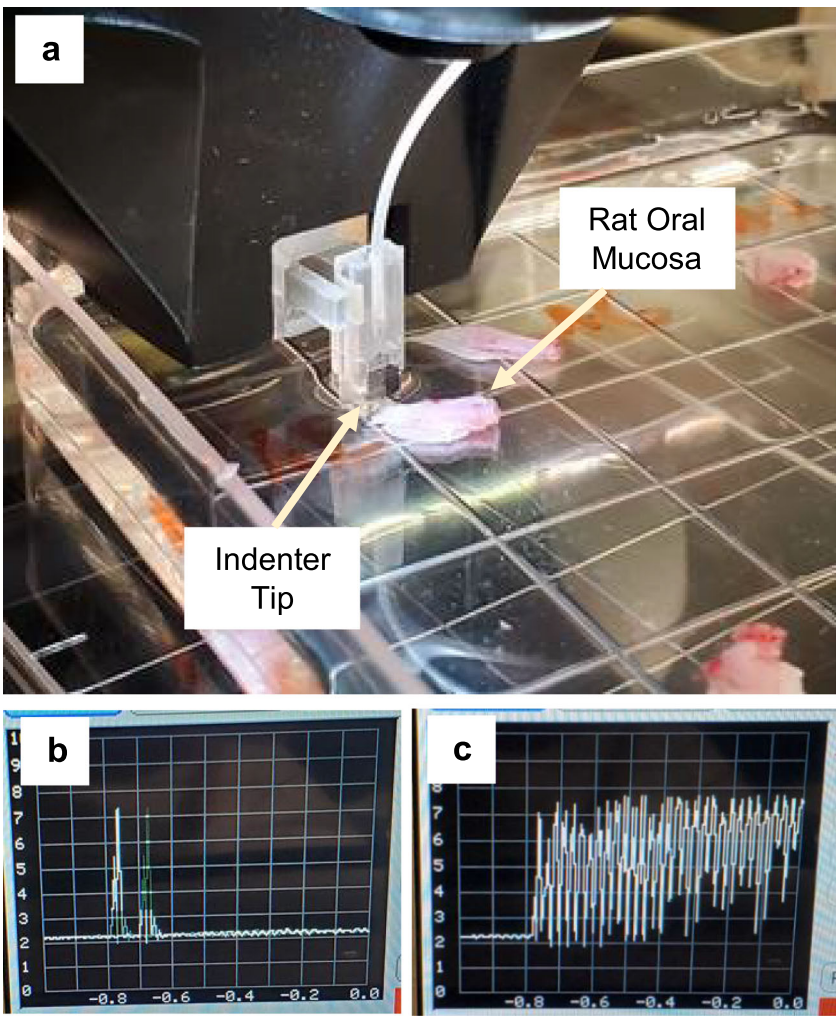

Fig. 1 **a** An image of the setup to measure the biomechanical stiffness using the Piuma nanoindenter with indentation on the rat oral mucosa. **b** A scope image of the optical waveform showing a spike from movement of the probe, but no surface contact (rapid return to baseline). **c** A scope image of the optical waveform showing vibrational movement of the probe consistent with surface contact

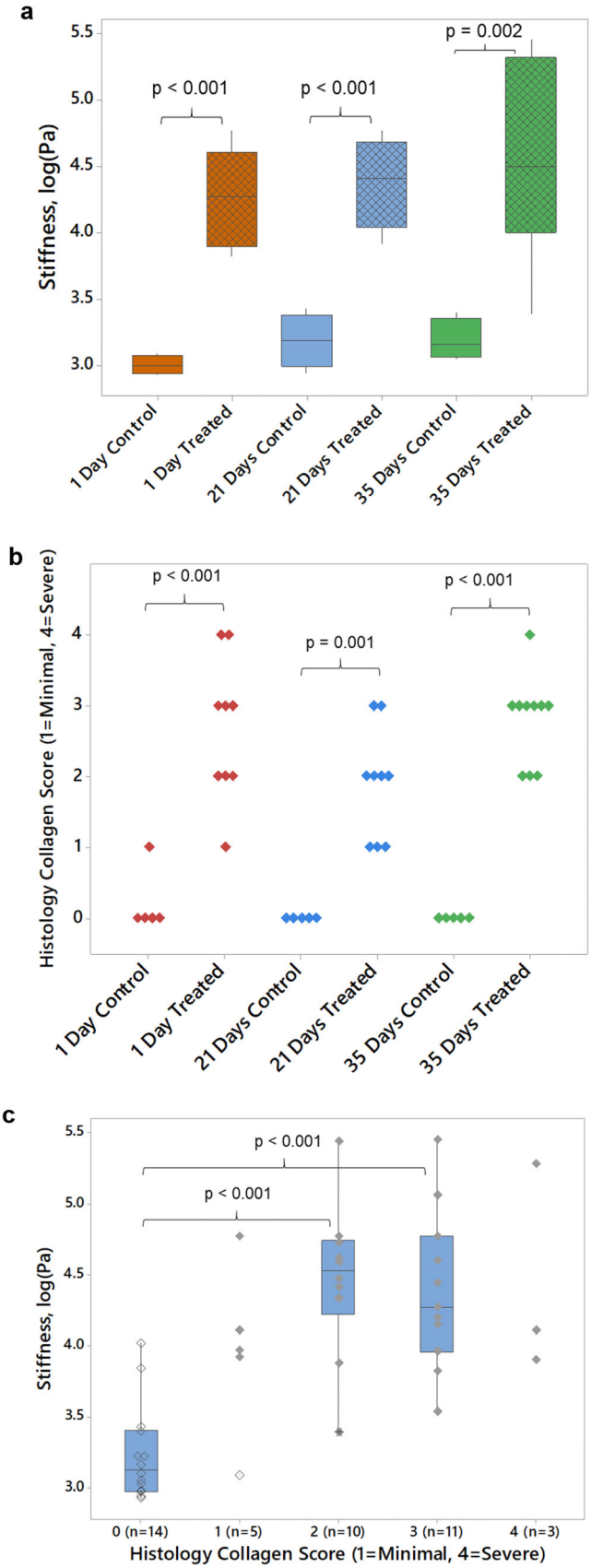

◀ **Fig. 2** **a** The biomechanical results represented by effective Young's modulus are shown on a logarithmic scale at day 1, day 21, and day 35 post-treatment ($n = 5$ for control group at each time point, $n = 10$ for treated group at each time point). At least an order of magnitude difference between laser-irradiated samples and controls was maintained over time. The treated groups were significantly different from the control groups, and all significant differences with their p values are shown. Boxes represent the interquartile range. **b** The histopathological results of collagen morphology are shown for all samples at day 1, day 21, and day 35, with p values where significant differences were found. **c** The biomechanical stiffness value for each animal is plotted against its histopathological collagen score, for the entire data set. Open circles represent control animals, and filled circles represent treated animals. Statistical differences are shown with their p values. Boxes represent the interquartile range, where sample count was adequate for statistics

variance and uneven sample size between groups, Welch's ANOVA was performed on the data with Games-Howell pairwise comparisons between groups.

Results

All of the treated and control animals maintained normal weight (adjusted for age and gender) during the study period, and no abnormalities or significant adverse effects were observed. All animals resumed normal eating and drinking habits after the effects of anesthesia dissipated.

The tissue biomechanical stiffness data, measured as effective Young's Modulus, is shown in Fig. 2a. The mean stiffness values for the control groups were 1.0 ± 0.17 kPa at day 1, 1.7 ± 0.17 kPa at day 21, and 1.6 ± 0.63 kPa at day 35. No significant difference was found between the three control groups ($p > 0.05$). The mean stiffness values for the treatment groups were 25 ± 18 kPa for day 1, 29 ± 19 kPa for day 21, and 97 ± 113 kPa for day 35. No significant difference was found between the three treated groups ($p > 0.05$). The increase in stiffness of the treated animal tissues was maintained at over an order of magnitude over that of the controls ($p \leq 0.002$ for each time point).

Collagen histopathological data is shown in Fig. 2b. One test sample at day 1 and one test sample at day 21 were damaged during processing, so these two samples were not represented in the data set. The mean collagen histopathological values for control groups were 0.20 ± 0.45 for day 1 and 0 for days 21 and 35. No significant difference was found between the three control groups ($p > 0.05$). The mean collagen histopathological values for the treated groups were 2.7 ± 1.0 for day 1, 1.9 ± 0.78 for day 21, and 2.8 ± 0.63 for day 35. No significant difference was found between the three treated groups ($p > 0.05$). An overall change from baseline persisted through the inflammation stage (day 1) and into the tissue remodeling stages (days 21 and 35), where a moderate accumulation of collagen was noted in the lamina propria,

indicative of the formation of a maturing fibrosis under the epithelium. There were significant differences between the treated groups and the control groups ($p \leq 0.001$) at each time point.

Histopathological changes in collagen coincided with the observed increase in tissue stiffness for all time points. For each animal, its biomechanical stiffness value was plotted against its histopathological collagen score across the entire data set, as shown in Fig. 2c. The general trend was an increase in stiffness as histopathological collagen score increases. Statistical differences were found between a score of 0 and a score of 2 ($p < 0.001$) or 3 ($p < 0.001$). Statistical values comparing animals with scores of 1 and 4 were not meaningful due to low sample counts for those scores. Furthermore, one control sample had a score of 1, which skewed the average stiffness down for animals with a score of 1. Higher sample counts would be needed to demonstrate significant differences between scores 1–4. Additional attempts to distinguish the data by time point for this analysis did not affect the outcome of the results.

Examples of the histopathological images at days 1, 21, and 35 of the study are shown in Fig. 3. Control animals at all three time points exhibited normal organization of lamina propria collagen, characterized by densely arranged thick bundles running parallel to the epithelial surface, the submucosal adnexa consisting of less densely arranged collagen fibers, and epithelia intact with normal stratification of epithelial cell layers. At day 1, in response to laser irradiation, mild-to-moderate inflammation was observed, including some areas of mild focal epithelial erosion/ulceration and minimal necrosis in some samples. However, these were resolved in time, and no abnormal inflammation markers were noted at days 21 and 35.

A mild-to-severe disruption of the lamina propria collagen with shorter bundles was noted at day 1, occurring with signs of tissue contraction. At day 21, occasional mild focal epithelial hyperplasia was noted in some samples. In all treated samples at day 21, there was an observed increased density of collagen bundles in the lamina propria not organized parallel to the epithelial surface, which is indicative of a maturing fibrosis. At day 35, an increased density and thickness of lamina propria collagen bundles running parallel to the epithelial surface was observed, with a similar effect in the submucosal collagen in some samples. For all treated samples, the overall thickness of the connective tissue layers increased compared with controls, which was indicative of mature fibrotic tissue in response to laser irradiation.

Discussion

Other lasers have been used with the aim of stiffening oral tissues using lasers with relatively low fluence, but a quantitative measure of stiffness on irradiated tissues has not been demonstrated to our knowledge. Using a 9.3-μm CO_2 laser, this study has demonstrated a quantitative measure of increased stiffness to the soft palate in vivo and corroborated it with histopathological outcomes. Other than collagen changes (contraction and accumulation), there were no reported lasting effects on the tissues after day 1. A mild-to-moderate inflammation response and minimal signs of necrosis were reported at day 1 but was not surprising, since the tissues were disrupted by heat from the laser, and heat-shock proteins may be activated, particularly in the superficial epithelium [7, 17]. A complete re-epithelization occurred by the day 21 time point for any areas that may have had epithelial erosion, so there was no irreversible damage to the basal membrane that may lead to unhealed surface changes. Furthermore, the rats in this study had no significant adverse effects reported on behavioral or signs of pain, even immediately after dissipation of anesthesia following the treatment. This demonstrates that the 9.3-μm CO_2 laser can be safely used for an oral tissue contraction procedure in patients, with minimal undesired effects post-treatment.

Previous reports demonstrated that a fairly large spherical tip can measure the average stiffness for bulk tissue over a broad depth and width relative to the indentation size [18, 19]. Here, using a spherical probe, we found that 9.3-μm CO_2 laser irradiation caused a contraction of the tissue that increased bulk tissue stiffness by more than an order of magnitude, which is important because this suggests that the results are beyond inherent tissue and measurement variability [16, 20]. More importantly, the increased stiffness of the tissue, caused initially by the contraction/disruption of collagen, persisted through the inflammatory phase and into the tissue remodeling phase, rather than softening or breaking down as the tissue changed structure. Over time, collagen was recruited, causing a thickening of the lamina propria, which was indicative of a maturing fibrosis. This fibrosis-like formation may be the desired result to provide a lasting benefit in the reduction of snoring vibrations.

The corroboration of histopathological data with the biomechanical data helped to confirm a pair of hypotheses. The first was that the changes in tissue stiffness were caused by the observed changes in collagen in the subepithelial oral mucosa layers, and the second was that biomechanical indentation can assess these subsurface tissue mechanical properties across all time points. A study with a larger number of samples could better demonstrate any statistically significant differences that may occur between the ranked histopathological scores and continuous biomechanical data. However, correlations between such data sets are inherently difficult due to the large variability in biological samples, particularly in vivo.

At day 1, contracted collagen may contribute directly to the stiffness changes by relaxing the tissue into a configuration where the proteins' exposed amino acids bind to nearby

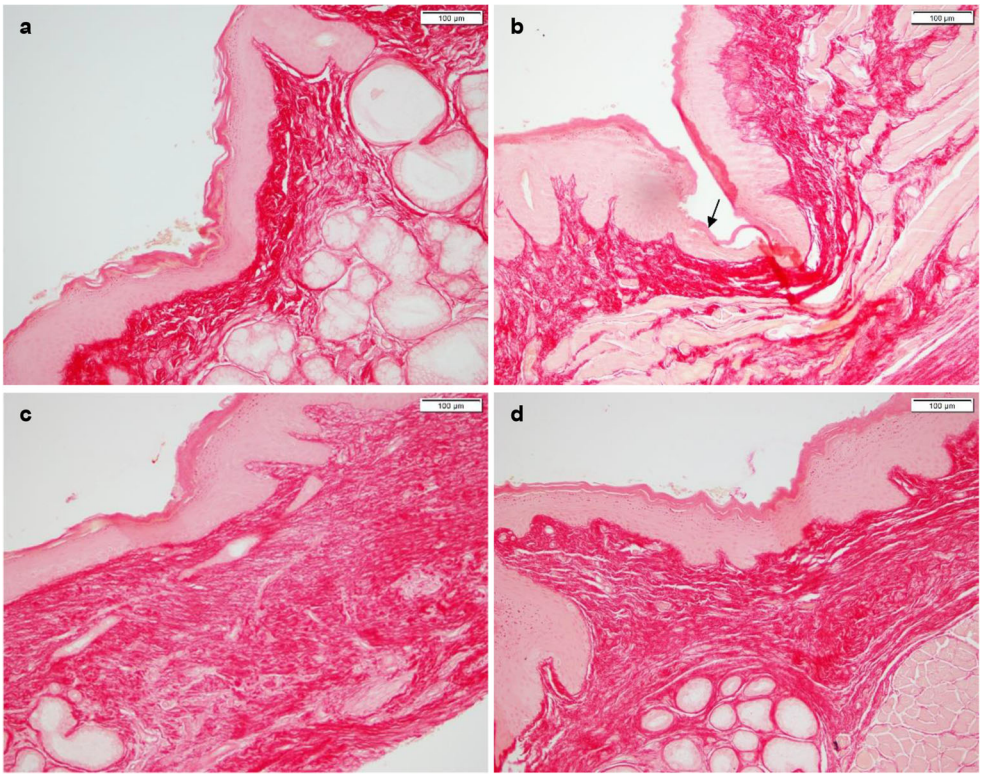

Fig. 3 **a** An example of a histopathological image for an untreated control soft palate tissue, stained with Sirius Red dye to highlight tissue collagen, showing normal organization of lamina propria collagen, becoming less dense in the submucosa. **b** Histopathological image of a sample from the day 1 post-treatment group showing a mild focal erosion of epithelium (arrow), with mild-to-moderate disruption of underlying lamina propria collagen structure in contracted tissue. **c** Histopathological image for a sample from the day 21 post-treatment group showing disorganized collagen bundles extending from the lamina propria into the submucosa. **d** Histopathological image for a sample from the day 35 post-treatment group showing increased density and thickness of lamina propria collagen bundles running parallel to epithelial surface

structures randomly. Later, accumulated collagen likely causes a continued increase in stiffness, possibly resulting from a formation of a subepithelial scar-like fibrosis, which is consistent with reports in skin tightening methods [21, 22]. In the soft palate, a scar-like fibrosis or a general tissue stiffening would be expected to reduce mechanical pliability of the mucosa, which would result in a reduction in tissue vibrations and thus snoring. Clinical studies have been performed to assess a reduction in snoring using an Er:YAG laser, but the results were highly variable and showed a significant reduction in outcome over time, requiring multiple re-treatments [9, 23]. Furthermore, histopathological tissue-level details were lacking, and it can be reasoned that problems with the treatment longevity may be related to the fairly shallow absorption depth of the Er:YAG laser. Conversely, the 9.3-μm CO_2 laser has a relatively deeper penetration depth, which enables subepithelial tissue to be targeted safely, to provide an effective treatment with potentially a single session.

The results of this study demonstrated that with a single treatment of the 9.3-μm CO_2 laser, soft palate biomechanical changes persisted into the remodeling phase over 35 days. This is indicative of changes that are expected to provide a lasting increase in stiffness over a long timeframe, likely > 1 year, which is based on the duration of the fibrosis or otherwise altered collagen structure. Since snoring is a vibration-dependent phenomenon, a concomitant reduction of snoring is expected. A clinical study is needed to prove directly that this increase in stiffness from CO_2 laser irradiation can decrease the incidence of snoring in patients over such a time frame.

Conclusion

In an in vivo animal study, soft palate contraction and wound healing response following non-ablative 9.3-μm CO_2 laser irradiation were measured by collagen histopathology and biomechanical stiffness. At all three time points (days 1, 21, and 35 post-treatment), the treated group with laser irradiation showed a significant increase in collagen contraction/disruption and accumulation and over an order of magnitude increase in stiffness, over the control group. These effects were well-tolerated with minimal signs of undesired damage that resolved quickly. This study indicates that irradiation at this wavelength can safely and effectively contract tissue in the upper airway to provide an increase in stiffness over a long period of time.

Acknowledgments Dr. Xin Brown of Boston University provided access to the device used in the biomechanics portion of this study and helped to train the authors on the use of nanoindentation. She also provided some idea of the initial indentation parameters that might work for this method on soft tissues. Dr. Gregory Rybacki of Toxikon, Inc., provided the histopathology analysis of the oral mucosa.

Funding information This study was funded by Convergent Dental.

Data availability The individual data can be provided per request.

Compliance with ethical standards

Conflict of interest The authors declare that they have no conflict of interest.

Ethical approval This study did not unnecessarily duplicate previous testing and that there were no non-animal alternatives acceptable for the evaluation of the test article as defined by the protocol. No evidence of pain and distress was reported to the Veterinarian or Study Director. Toxikon strictly adhered to the following standards in maintaining the animal care and use program:

United States Department of Agriculture (USDA), Animal and Plant Health Inspection Service, 9 CFR Ch. 1, Subchapter A-Animal Welfare.

"Guide for the Care and Use of Laboratory Animals," National Research Council, 2011.

Office for Laboratory Animal Welfare (OLAW), "Public Health Service Policy on Humane Care and Use of Laboratory Animals," Health Research Extension Act of 1985 (Public Law 99–158 November 20, 1985), Revised 2015.

ISO 109932, 2006, Biological Evaluation of Medical Devices Part 2: Animal Welfare Requirements.

AAALAC International accreditation.

References

1. Wang Z, Rebeiz EE, Shapshay SM (2002) Laser soft palate stiffening: an alternative to uvulopalatopharyngoplasty. Lasers Surg Med 30(1):40–43 http://www.ncbi.nlm.nih.gov/pubmed/11857602. Accessed February 20, 2019
2. Kirsch KM, Zelickson BD, Zachary CB, Tope WD (1998) Ultrastructure of collagen thermally denatured by microsecond domain pulsed carbon dioxide laser. Arch Dermatol 134(10):1255–1259. https://doi.org/10.1001/archderm.134.10.1255
3. Fitzpatrick RE, Rostan EF, Marchell N (2000) Collagen tightening induced by carbon dioxide laser versus erbium: YAG laser. Lasers Surg Med 27(5):395–403. https://doi.org/10.1002/1096-9101(2000)27:5<395::AID-LSM1000>3.0.CO;2-4
4. da Cunha MG, Paravic FD, Machado CA (2015) Histological changes of collagen types after different modalities of dermal remodeling treatment: a literature review. Surg Cosmet Dermatol 7(4):285–291. https://doi.org/10.5935/scd1984-8773.2015741
5. Ross EV, Yashar SS, Naseef GS et al (1999) A pilot study of in vivo immediate tissue contraction with CO2 skin laser resurfacing in a live farm pig. Dermatologic Surg 25(11):851–856. https://doi.org/10.1046/j.1524-4725.1999.99091.x
6. Von Den Hoff JW, Maltha JC, Kuijpers-Jagtman AM (2006) Palatal wound healing: the effects of scarring on growth. In: Cleft Lip and Palate. Springer Berlin Heidelberg, Berlin, pp 301–313. https://doi.org/10.1007/3-540-30020-1_20
7. Krysztof Miracki ZV (2013) Nonsurgical minimally invasive Er: YAG laser snoring treatment. J Laser Heal Acad 1(1):36–41
8. Sippus J (2015) NightLase procedure – laser snoring and sleep apnea reduction treatment. J Laser Heal Acad 2015(1):S06
9. Cetinkaya EA, Turker M, Kiraz K, Gulkesen HK (2016) Er: Yag laser treatment of simple snorers in an outpatient setting. Orl. 78(2):70–76. https://doi.org/10.1159/000443510
10. Green J, Weiss A, Stern A (2011) Lasers and radiofrequency devices in dentistry. Dent Clin N Am 55(3):585–597. https://doi.org/10.1016/j.cden.2011.02.017
11. Fantarella D, Kotlow L (2014) The 9.3-μm CO 2 dental laser: technical development and early clinical experiences. J Laser Dent J Laser Dent 2222(11):10–27
12. Berger G, Finltelsteln Y, Oplnr D (1999) Histopathologic changes of the soft palate after laser-assisted uvulopalatoplasty. Arch Otolaryngol Head Neck Surg 125(7):786–790. https://doi.org/10.1001/archotol.125.7.786
13. Berger G, Finkelstein Y, Stein G, Ophir D (2001) Laser-assisted uvulopalatoplasty for snoring: medium- to long-term subjective and objective analysis. Arch Otolaryngol Head Neck Surg 127(4):412–417. https://doi.org/10.1001/archotol.127.4.412
14. Lalabonova H, Ilieva EM (2013) Clinical evaluation of the healing process of oral soft tissue surgical wounds stimulated by low-level laser therapy. J IMAB - Annu Proceeding 19(2):279–281. https://doi.org/10.5272/jimab.2013192.279
15. Poyrazoğlu E, Doğru S, Saat B, Güngör A, Çekin E, Cincik H (2006) Histologic effects of injection snoreplasty and radiofrequency in the rat soft palate. Otolaryngol Head Neck Surg 135(4):561–564. https://doi.org/10.1016/j.otohns.2006.05.008
16. Fung Y (2013) Biomechanics: mechanical properties of living tissues. Springer Science & Business Media, New York
17. Song AS, Najjar AM, Diller KR (2014) Thermally induced apoptosis, necrosis, and heat shock protein expression in 3D culture. https://doi.org/10.1115/1.4027272
18. Akhtar R, Schwarzer N, Sherratt MJ et al (2009) Nanoindentation of histological specimens: mapping the elastic properties of soft tissues. J Mater Res 24(03):638–646. https://doi.org/10.1557/jmr.2009.0130
19. Qian L, Zhao H (2018) Nanoindentation of soft biological materials. Micromachines. 9(12):654. https://doi.org/10.3390/mi9120654
20. McKee CT, Last JA, Russell P, Murphy CJ (2011) Indentation versus tensile measurements of Young's modulus for soft biological tissues. Tissue Eng Part B Rev 17(3):155–164. https://doi.org/10.1089/ten.TEB.2010.0520
21. Seckel BR, Younai S, Wang KK (1998) Skin tightening effects of the ultrapulse CO2 laser. Plast Reconstr Surg 102(3):872–877. https://doi.org/10.1097/00006534-199809030-00040
22. Sasaki GH (2010) Quantification of human abdominal tissue tightening and contraction after component treatments with 1064-nm/1320-nm laser-assisted lipolysis: clinical implications. Aesthetic Surg J 30(2):239–245. https://doi.org/10.1177/1090820X10369373
23. Svahnström K (2013) Er : YAG laser treatment of sleep-disordered breathing. J laser Health Acad 2013(2):13–16